Australian Journal of Basic and Applied Sciences, 4(8): 3467-3483, 2010
ISSN 1991-8178

Experimental and Analytical Analysis for Flow around a Rotating Circular Cylinder Suddenly Set into Motion

[1,5]Muhammed Sohel Rana, [2]Muhammad Nasimul Hoque, [2]Nasrin Akter, [3]Hossain Mohammed Farabi and [4]Mohammed Asaduzzaman

[1]Central Engineering Facilities, Atomic Energy Research Establishment, Bangladesh Atomic Energy Commission, Bangladesh;
[2]Dept. of Mathematics, School of Physical Science, Shahjalal University of Science & Technology, Sylhet-3114, Bangladesh;
[3]3 Bangla Link Telecom, Bangladesh;Network Deployment (Transmission), Bangla Link (Orascom Telecom Company), Bangladesh;
[4]Walton Hi-Tech Industries Ltd., Jiban Bima Bhaban (Level-3), 10, Dilkusha Commercial Area, Dhaka – 1000, Bangladesh;
[5]Mechanical Systems Engineering, Faculty of Engineering, University of the Ryukyus, Okinawa, Japan.

Abstract: We report on analytical and experimental analysis of the velocity profile that causes suddenly starts rotating cylinder. In this study, the incompressible unsteady flow around a fixed rotating circular cylinder with finite length 150 mm was analyzed by two different exact analytical solutions of the unsteady Navier-Stokes equations. The first one (Equation (13)) is obtained by complimentary error function and the second one (Equation (17)) is obtained by Bessel's function of first and second kind that was earlier known solution Coster (1919). Unsteady exact solution for suddenly moving cylinder was presented and compared with available experimental data. Special Attention was given to compare analytical solution and experimental results and finally recommend to first analytical solution. Experiment treats the unsteady flow generated by a solid circular cylinder of 30 mm of diameter. In experiment, cylinder was rotated at four different rpm such as 25, 50, 75, 100 rpm. Movies were taken to measure velocity around a suddenly starts rotating cylinder after 198s. After compared with experimental results and two analytical results we recommend both analytic solutions for different time stipulation for suddenly starts rotating circular cylinder.

Key words: Rotating circular cylinder, unsteady flow, viscous flow, suddenly starts, Navier-Stokes Equations.

INTRODUCTION

The Flow around a rotating circular cylinder is a popular test case for computational fluid dynamics and an important prototype for separated flows. In the study of unsteady flow over a rotating circular cylinder, there are basic mechanisms, which are still not fully understood. However, it is a complex, unsteady flow that can be quite difficult to compute accurately. Coster (1919) have investigated flow around a rotating circular cylinder in the past few decades. Most of these efforts are based on numerical simulation, laboratory experiments, and very few on analytical techniques. Unsteady flows, laminar and turbulent, are encountered in various industrial, bio-medical, and environmental applications. Among examples are flows in turbomachinery, microdevices, internal combustion engines, etc. Detailed study of physics of such flows is of intrinsic value. The potential flow over a rotating cylinder in a uniform stream plays an important role in classical airfoil theory in which the flow and airfoil shape is obtained by conformal transformation.

For some unsteady flows, the exact solution of Navier-Stokes equations is known (Coster, 1919; Schlichting and Gersten, 2000; Chia-*Shun*, 1969) and therefore, the flow pattern can be obtained analytically. One of them is the solution of the rotating circular cylinder, which was an unsteady flow around a suddenly rotates circular cylinder (Johnson and Richard, 1998; Coster, 1919). Analysis of the Stokes solution yields

Corresponding Author: Muhammad Nasimul Hoque, Dept. of Mathematics, School of Physical Science, Shahjalal University of Science & Technology, Sylhet-3114, Bangladesh
Email: nhhoquesust@gmail.com

valuable insight into physics of the flow. In a previous paper by Collins & Dennis (1973), a method was given for solving the Navier-Stokes equations at high Reynolds numbers to determine the initial flow past a circular cylinder impulsively started translating from rest. In essence, the method was based on an expansion procedure in terms of powers of a parameter $k = 2(2t/R)^{0.5}$, where t was a suitably scaled time measured from the start of the motion and R = $2Ua/u$ was a Reynolds number. Here a is the radius of the cylinder, U the constant velocity with which it is set in motion, and u is the coefficient of kinematic viscosity of the fluid.

An interesting work by Benton (1966) studied the impulsive rotation from rest of a disk in an infinite viscous fluid. Assuming the time scale is small, Benton expanded the unknowns in power series in time. The unsteady Navier-Stokes equations then become decoupled for each successive order of the time variable. Benton solved for the first two orders analytically, and then numerically computed the next two orders. Although such a method was used to treat impulsive start problems before, what is significant is the way Benton presented the small-time results. He plotted, on the same graph, the solutions of various different orders in time. The range of validity of the solutions up to order N was determined by observing the location where the solution of order N +1 bifurcated. This is equivalent to the quantitative error estimation of an asymptotic series. Benton showed that the solution up to the fourth order was valid for small" normalized times as large as 1.5, at which time the stresses and velocities were very close to the steady state values of the classical Von Karman rotating disk problem. Thus in certain transient problems the solution for small times may infer the steady state.

However, inferring flow physics from exact solutions is not always an easy task, especially when a solution involves special functions. The solution in unsteady parallel flow for flat plate (Schlichting and Gersten, 2000), is an example, which was Stokes first problem. After Coster (1919) any detailed analysis for suddenly rotates cylinder has not been made yet and is the prime objective of the present paper. Such analysis is important, for instance, for understanding the behaviors of stationary vortex pair.

Our concern is with the stability of the unsteady viscous flow of an incompressible fluid in a suddenly rotates circular cylinder. Cylindrical geometries often appear in engineering structures. Although these structures are very simple, the fluid flow around them is not. Frequently exact solutions of the unsteady Navier-Stokes equations exist when there are already exact solutions of the corresponding steady flow at hand. Examples of unsteady flows are "start-up" flows from rest, or "shut-down" flows where the flow dies away in time. A characteristic of the flows considered in what follows is what the unsteady parts of the velocity are independent of the coordinate θ parallel to the cylinder wall. Because of this, the simplifications to the Navier-Stokes equations are so great that exact solution can be determined. Interest in this problem arises not only from the point of view of basic fluid mechanics but also from its applications to flow control. There are numerous methods available for the solution of the Navier-Stokes equations such as the finite difference, finite element, analytical, finite volume and spectral methods. In this paper, we look at two analytical methods for abruptly start rotating circular cylinder.

It was the aim of the present study to compare analytical results with experimental results the incompressible flow field over a suddenly rotates circular cylinder and to recommend these two exact solution in different time condition.

Governing Equation for Both Analytical Solution:

In this section, the formulation for solving two-dimensional incompressible Navier-Stokes equations and continuity equation in cylindrical coordinates is given. The formulation and the analytical methods described in this section are derived for suddenly start rotating circular cylinder problem, but it is valid for general viscous flow. The first section describes the formulation of the general governing equations for analytical methods, and the later section initial and boundary conditions. The last section presents the details methods of solution.

`We consider an incompressible flow confined around a cylinder (the flow between two concentric cylinders can be handled with a similar technique, and is in fact easier to deal with because of the absence of the coordinate singularity), i.e., the domain in cylindrical coordinates are r, θ and z. The equations governing the flow are Navier–Stokes, together with initial and boundary conditions.

The non-dimensionalized equations in three-dimensional cylindrical coordinates are the continuity equation is

$$\frac{\partial v_z}{\partial z} = 0 \tag{1}$$

Then, the Navier–Stokes equations in velocity-pressure formulation written in cylindrical coordinates are

$$r-component:\ \rho\left(\frac{\partial v_r}{\partial t}+v_r\frac{\partial v_r}{\partial r}+\frac{v_\theta}{r}\frac{\partial v_r}{\partial \theta}+v_z\frac{\partial v_r}{\partial z}-\frac{v_\theta^2}{r}\right)$$
$$=-\frac{\partial p}{\partial r}+\mu\left(\frac{\partial^2 v_r}{\partial r^2}+\frac{1}{r}\frac{\partial v_r}{\partial r}-\frac{v_r}{r^2}+\frac{1}{r^2}\frac{\partial^2 v_r}{\partial \theta^2}+\frac{\partial^2 v_r}{\partial z^2}-\frac{2}{r^2}\frac{\partial v_\theta}{\partial \theta}\right)+F_r \tag{2}$$

$$\theta-component:\ \rho\left(\frac{\partial v_\theta}{\partial t}+v_r\frac{\partial v_\theta}{\partial r}+\frac{v_\theta}{r}\frac{\partial v_\theta}{\partial \theta}+v_z\frac{\partial v_\theta}{\partial z}+\frac{v_r v_\theta}{r}\right)$$
$$=-\frac{\partial p}{\partial \theta}+\mu\left(\frac{\partial^2 v_\theta}{\partial r^2}+\frac{1}{r}\frac{\partial v_\theta}{\partial r}-\frac{v_\theta}{r^2}+\frac{1}{r^2}\frac{\partial^2 v_\theta}{\partial \theta^2}+\frac{\partial^2 v_\theta}{\partial z^2}+\frac{2}{r^2}\frac{\partial v_r}{\partial \theta}\right)+F_\theta \tag{3}$$

$$z-component:\ \rho\left(\frac{\partial v_z}{\partial t}+v_r\frac{\partial v_z}{\partial r}+\frac{v_\theta}{r}\frac{\partial v_z}{\partial \theta}+v_z\frac{\partial v_z}{\partial z}\right)$$
$$=-\frac{\partial p}{\partial z}+\mu\left(\frac{\partial^2 v_z}{\partial r^2}+\frac{1}{r}\frac{\partial v_z}{\partial r}+\frac{1}{r^2}\frac{\partial^2 v_z}{\partial \theta^2}+\frac{\partial^2 v_z}{\partial z^2}\right)+F_z \tag{4}$$

The mathematical problem that we have solved might be considered as the two-dimensional flow generated by a fixed infinitely long cylinder whose axis coincides with the *z*-axis placed in a viscous incompressible fluid. To commence the mathematical solution we assume that the velocity $v_\theta(r, t)$ is a function of *r* and *t* only. The continuity equation is satisfied by this assumption. For 2-Dimensional unsteady flow and no external force,

$$v_\theta \neq 0, \quad v_r = v_z = 0 \quad and \quad \frac{\partial p}{\partial \theta}=0$$

$$and \quad F_r = F_\theta = F_z = 0$$

From equation (1) and (2) we get,

$$\frac{1}{r}\frac{\partial v_\theta}{\partial \theta}=0 \tag{5}$$

$$\frac{\partial p}{\partial r}=\frac{\rho\,\mathrm{v}_\theta^2}{\mathrm{r}} \tag{6}$$

It is considered that equation (6) is differentiated by θ,

$$\frac{\partial^2 p}{\partial r\,\partial \theta}=\frac{2\,p v_\theta}{r}\frac{\partial v_\theta}{\partial \theta}=0$$

$$\frac{\partial p}{\partial \theta}=0 \tag{7}$$

The governing equations are the unsteady Navier-Stokes equations. We treat a start-up flow, i.e. motion from rest. We consider the flow close to the cylinder wall, which is suddenly set into motion with a constant velocity $a\Omega$ in its own plane. This problem was first solved by Coster (1919).

Consider that special case of a viscous fluid near cylinder wall that is set suddenly in motion. The unsteady two dimensional Navier-Stokes equations reduces to

$$\frac{\partial v_\theta}{\partial t} = \upsilon\left(\frac{\partial^2 v_\theta}{\partial r^2} + \frac{1}{r}\frac{\partial v_\theta}{\partial r} - \frac{v_\theta}{r^2}\right) \tag{8}$$

Equation (8) is identical with the equation of radial flow of heat in two dimensional unsteady temperature fields *T(r, t)*. There are therefore many solutions to this type of differential equation in the literature on heat conduction (Carslaw and Jaeger 1959; Grigull and Sandner 1986).

Initial and Boundary Conditions for 1st Solution:

For the system, $v_\theta = v_\theta(r,t);\ v_r = 0;\ v_z = 0$

The initial condition for the fluid that starts from rest is given as:

Initial Condition $t \le 0 \quad for\ all\ r: \qquad v_\theta = 0$

The corresponding boundary conditions for first solution are:

Boundary Condition, $t > 0:\ r = a: \qquad v_\theta = a\Omega$

$r = \infty: \qquad v_\theta = 0$

From the *Π* theorem in dimensional analysis if follows that $v_\theta/a\Omega = f(r/(t\upsilon)^{1/2})$. Indeed. By introducing the dimensionless similarity variable defining,

$$\varphi = \varphi(\eta) \qquad \eta = \frac{r}{(4\upsilon t)^{\frac{1}{2}}}$$

Dimensionless velocity, $\varphi = \dfrac{v_\theta}{a\Omega}$

From equation (8), we get new equation,

$$\frac{\partial \varphi}{\partial t} = \upsilon\left(\frac{\partial^2 \varphi}{\partial r^2} + \frac{1}{r}\frac{\partial \varphi}{\partial r} - \frac{\varphi}{r^2}\right) \tag{9}$$

New Boundary and Initial Conditions are

New Boundary Condition, $t > 0:\ \eta = a: \quad \eta_1 = \dfrac{a}{(4\upsilon t)^{\frac{1}{2}}} \quad \varphi = 1$

New Boundary and Initial Condition, $\eta = \infty: \quad \varphi = 0$

First Analytic Solution:

$$\frac{\partial \varphi}{\partial t} = -\frac{\eta}{2t}\frac{\partial \varphi}{\partial \eta};\ \frac{\partial \varphi}{\partial r} = \frac{1}{\sqrt{4\upsilon t}}\frac{\partial \varphi}{\partial \eta};\ \frac{\partial^2 \varphi}{\partial r^2} = \frac{1}{4\upsilon t}\frac{\partial^2 \varphi}{\partial \eta^2}$$

Substituting above value in Equation (9), we find

$$\frac{1}{2}\frac{\partial^2\varphi}{\partial\eta^2}+(\frac{1}{2\eta}+\eta)\frac{\partial\varphi}{\partial\eta}-\frac{\varphi}{2\eta^2}=0 \tag{10}$$

Defining, $\psi = \dfrac{d\varphi}{d\eta}$

Now Equation (10) becomes

$$\frac{d\psi}{d\eta}=-2\eta\psi \tag{11}$$

From Equation (11), it follows that

$$\psi=C_1 e^{-\eta^2}$$

Second Integration

$$\varphi(\eta)=C_1\int_0^{\eta} e^{-\eta^2}\,d\eta + C_2 \tag{12}$$

where,

C_1, C_2 are integrating constant.
Introducing BCs in Equation (12)

$$C_1=-\frac{2}{(\pi)^{\frac{1}{2}}\ errc(\eta_1)}\ ,\ C_2=\frac{1}{erfc(\eta_1)}$$

Substituting these values in Equation (12) then becomes

$$\varphi = \frac{v_\theta(r,t)}{a\Omega} = \frac{erfc(\eta)}{erfc(\eta_1)} = \frac{erfc\left(\dfrac{r}{(4\upsilon t)^{\frac{1}{2}}}\right)}{erfc\left(\dfrac{a}{(4\upsilon t)^{\frac{1}{2}}}\right)}$$

Finally,

$$v_\theta(r,t) = a\Omega\,\frac{erfc\left(\dfrac{r}{(4\upsilon t)^{\frac{1}{2}}}\right)}{erfc\left(\dfrac{a}{(4\upsilon t)^{\frac{1}{2}}}\right)} \tag{13}$$

Initial and Boundary Conditions for 2nd Solution:

This problem was first solved by Coster (1919) The unsteady Navier-Stokes equations reduces to equation (8)

For the system, $v_\theta=v_\theta(r,t);\ v_r=0;\ v_z=0$

The boundary conditions for second solution are:
Boundary conditions

$v_\theta(r = a, t) = a\Omega$

$v_\theta(r = \infty, t) = 0$

and initial conditions are

$v_\theta(r > a, t = 0) = a\Omega$

$$\frac{\partial v_\theta(r \geq a, t = 0)}{\partial r} = 0$$

Second Analytic Solution:

We can solve the above equation with Variable Separation. For that,
Assume,

$v_\theta = f(r)g(t)$

$$f^{''}g + \frac{1}{r}f^{'}g - \frac{1}{r^2}fg = \frac{1}{\upsilon}fg^{'}$$

Let, $\frac{f''}{f} + \frac{1}{r}\frac{f'}{f} - \frac{1}{r^2} = \frac{1}{\upsilon}\frac{g'}{g} = -\lambda^2$

$$\frac{f''}{f} + \frac{1}{r}\frac{f'}{f} - \frac{1}{r^2} = -\lambda^2 \tag{14}$$

and

$$\frac{1}{\upsilon}\frac{g'}{g} = -\lambda^2 \tag{15}$$

Solving Equation (14) & (15) according to linear differential equation solution (Tenenbaum and Pollard, 1963), we get,

$$v_\theta(r,t) = \{AJ_1(r\lambda) + BY_1(r\lambda)\}e^{-\upsilon\lambda^2 t} + Cr + D\frac{1}{r} \tag{16}$$

Now we apply above boundary and initial conditions and for Eigenvalue Equation (16) finally appear in this form,

$$v_\theta(r,t) = \frac{a^2\Omega}{r} + \frac{2a\Omega}{\pi}\int_0^\infty e^{-\upsilon\lambda^2 t}\,\frac{J_1(r\lambda)Y_1(a\lambda) - J_1(a\lambda)Y_1(r\lambda)}{J_1^2(a\lambda) + Y_1^2(a\lambda)}\,\frac{1}{\lambda}\,d\lambda \tag{17}$$

MATERIALS AND METHODS

Experimental Apparatus and Methods:

The experiments were performed in an aquarium type circular device with a test section of 600 mm of radius, 800 mm of height (with stand) and height of 200 mm. Clear plastic sheets were fixed around all sides and bottom space. Top of this device is open. Black paints were coated inside around the wall and bottom wall. Solid aluminum cylinder (diameter 30 mm) with gear arrangement was fixed on the center of the black coated bottom wall. Gear arrangement was installed for control the cylinder rpm. The rotational speeds were measured by a tachometer, which was displayed in a digital display. The motion was transmitted to circular cylinder through gear arrangement by an asynchronous electric motor. Movie and still pictures were taken over open top of the device with the help of a steel stand. A small set of experiments described in the experimental apparatus and methods section that has shown in figure 1.

For experiment, device was filled by 150 mm height of water. The tracer particle (aluminum powder and 150 grain diameter meshes) was used for the visualization for stream the flow was started with the fluid at rest. To measure the velocity of the flow around the rotating cylinder small particles of lightweight material capable of floating such as aluminum dust were placed on free water surface. Velocities around the rotating cylinder were seen that as these particles move with the fluid they did rotate around cylinder axes, which was indicated by a line marked on the particle remaining parallel to itself during the different positions of the particles. We took movie pictures and still pictures at different rpm such as 25, 50, 75, and 100. To determine the linear velocity moving pictures were fallen on a large screen in scale 7:1 with the help of a multimedia projector then movie started through Windows Media Player. At the time of measure the velocity movie played very slowly within 1 second 30 frames were moved. Before started play fixed one point into the flow field from the cylinder wall subsequently movie was started and followed that fixed point. Finally, the distance by means of time traveled by that fixed point was measured. Linear velocities were calculated by measured distance and time. Above procedure was applied with different position from cylinder wall.

We also measured the particles direction, vortices distribution, and streamlines in the flow field with the assist of MatPIV v. 1.6.1. Particle Image Velocimetry (PIV) has seen a rapid growth over the last two decades, much owing to the developments in digital camera and solid-state laser technologies. PIV can essentially be looked upon as an application of pattern matching principles to experiments. We rely upon hardware such as lasers and cameras for illumination and image capture. Subsequently we use computer code to perform the pattern matching. MatPIV is one of a variety of different computer codes available written specifically for this purpose. We presented the graphical results from the experimental setup in result and discussion section.

RESULTS AND DISCUSSION

In this section, we will present graphical results that vary between experimental data and two analytic solutions result. Figure 2, 3, 4, 5 shows the still picture when cylinder rotated at 25, 50, 75, 100 rpm respectively. Experiments were carried out with 4 different rpm, 25, 50, 75, 100 rpm at same direction. The used equation for the calculation of the analytical velocity at t = 198s and same different rpm are equation (6) & equation (10) and it was compared with experimental data.

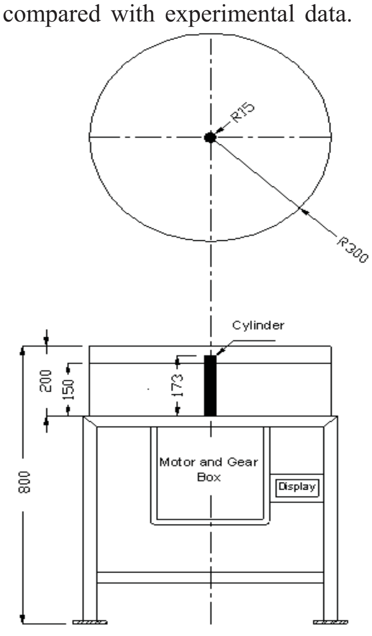

Fig. 1: Sketch diagram of Experimental Setup (mm).

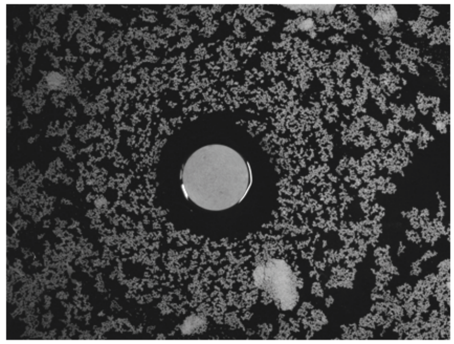

Fig. 2: Cylinder Rotates at 25 rpm, t = 198s

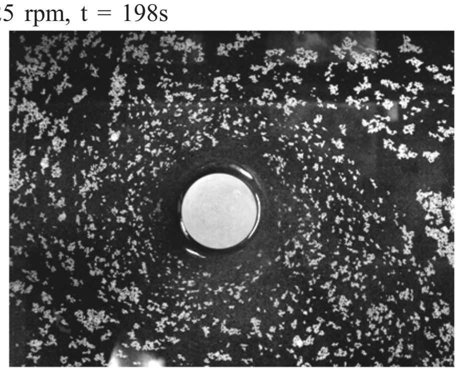

Fig. 3: Cylinder Rotates at 50 rpm, t = 198s

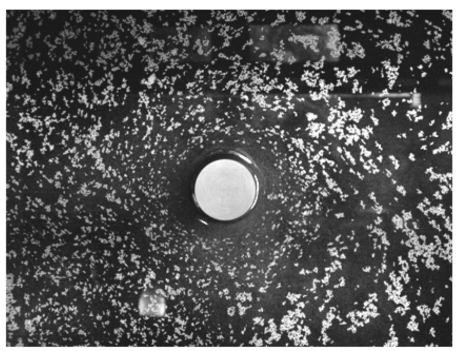

Fig. 4: Cylinder Rotates at 75 rpm, t = 198s

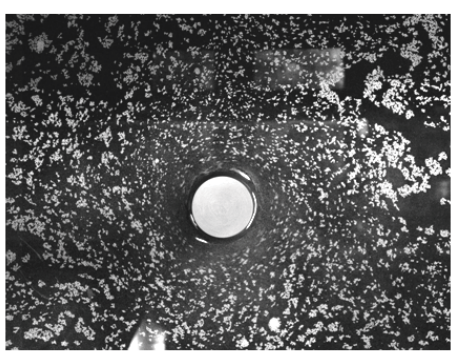

Fig. 5: Cylinder Rotates at 100 rpm, t = 198s

In figure 6 shows the velocity field whereat horizontal axes represents the distance from circular cylinder wall and vertical axes linear velocity distributions, 25 rpm, t = 198s. From this figure we marked that the velocity distribution before r = 3.5cm is below analytical results whereupon after 3.5cm it goes above analytical results. We may define this point as fluctuation point. In figure 7 this fluctuation point occurs at 3.5 cm but in figure 8 and figure 9 that point positioned at 4.0 cm and 4.5 cm respectively. From Figure 6 to 9 all graph have been compared with 1st analytic solution results with experimental results at 25, 50, 75, 100 rpm, t = 198s. From figure 10 to 13 have also been compared with second analytic solution results with experimental results at 25, 50, 75, 100 rpm, t = 198s. In figure 10 fluctuation, point appears at 3.75 cm whereupon in figure 11, 12 & 13 obtained at 4.25 cm, 4.4 cm & 4.75 cm respectively. Before fluctuation point experimental results below analytical results but reverse phenomena occurs after fluctuation point that marked in all graph. Before fluctuation point experimental results behind with analytical results whereas turbulent flow occurs from near cylinder wall to fluctuation point.

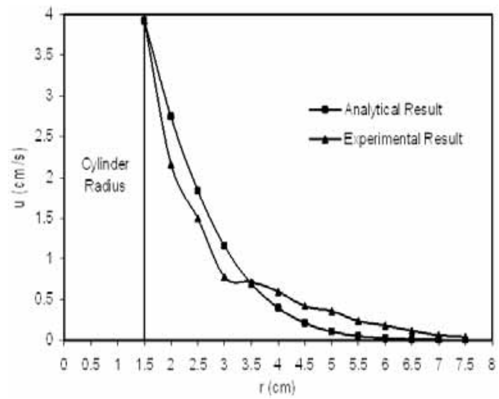

Fig. 6: Compare 1st Analytical solution with experimental results, 25 rpm, t = 198s

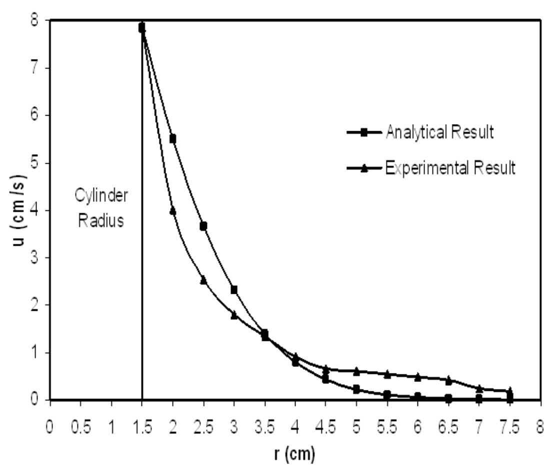

Fig. 7: Compare 1st analytical solution with experimental results, 50 rpm, t = 198s

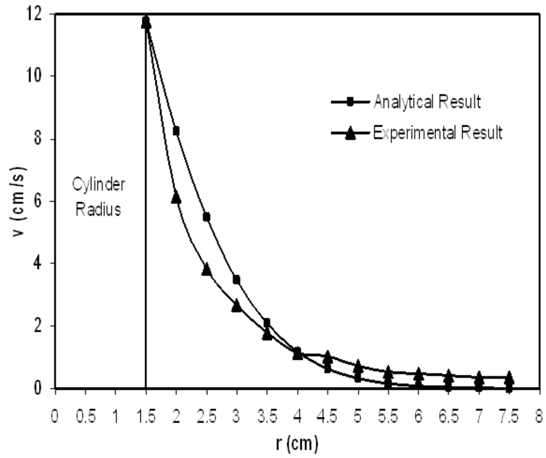

Fig. 8: Compare 1st analytical solution with experimental results, 75 rpm, t = 198s

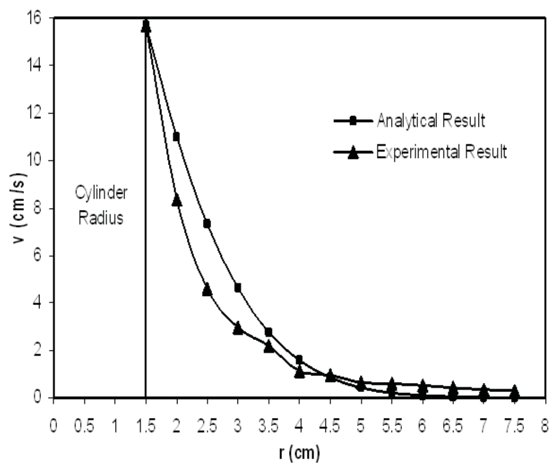

Fig. 9: Compare First analytic solution with experimental results, 75 rpm, t = 198s

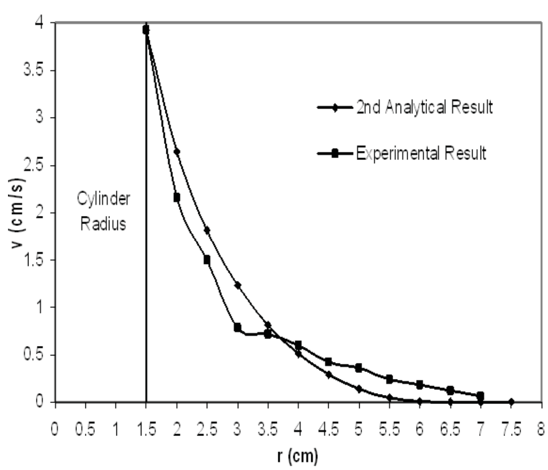

Fig. 10: Compare 2nd analytical solution with experimental results, 25 rpm, t = 198s

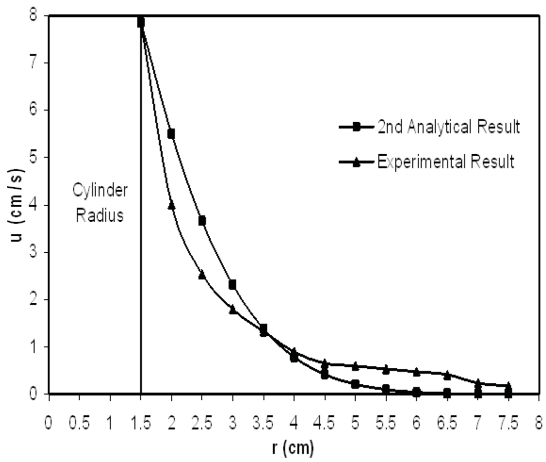

Fig. 11: Compare 2nd analytical solution with experimental results, 50 rpm, t = 198s

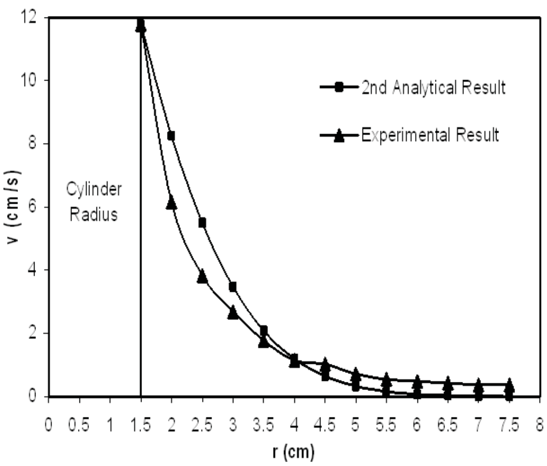

Fig. 12: Compare 2nd analytical solution with experimental results, 75 rpm, t = 198s

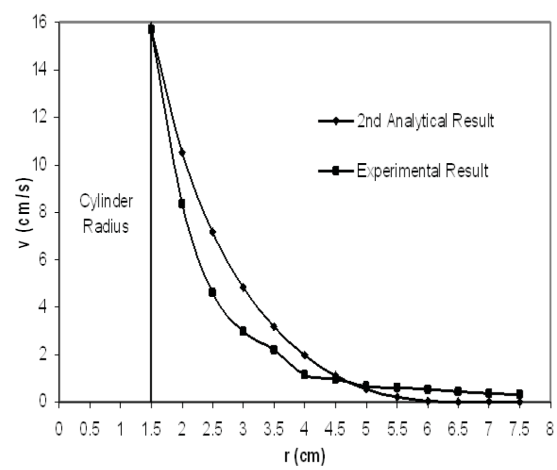

Fig. 13: Compare 2nd analytical solution with experimental results, 100 rpm, t = 198s

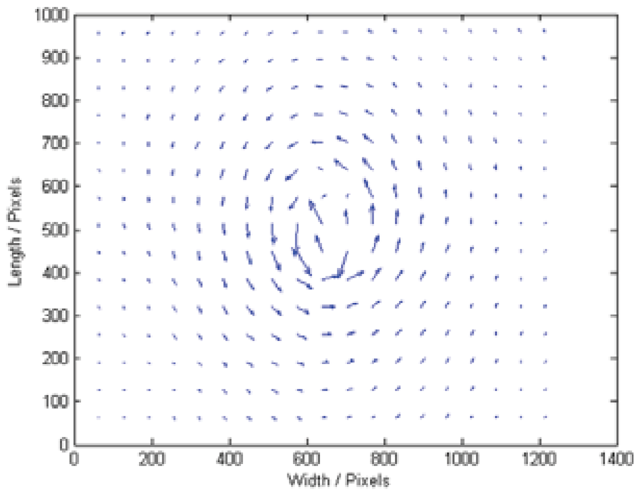

Fig. 14: Particle direction in the flow field for 25 rpm, t = 198s

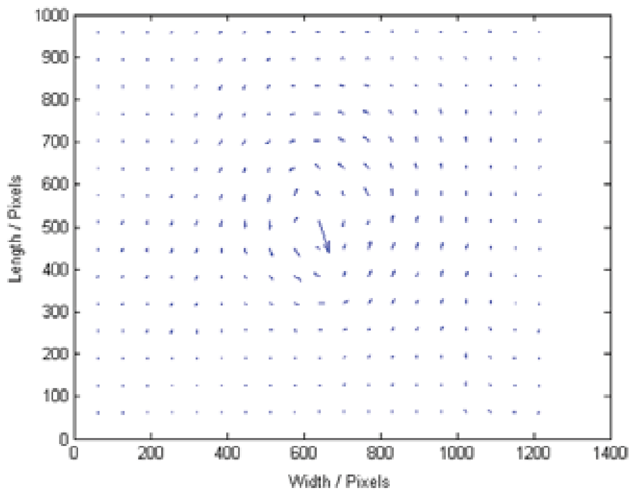

Fig. 15: Particle direction in the flow field for 50 rpm, t = 198s

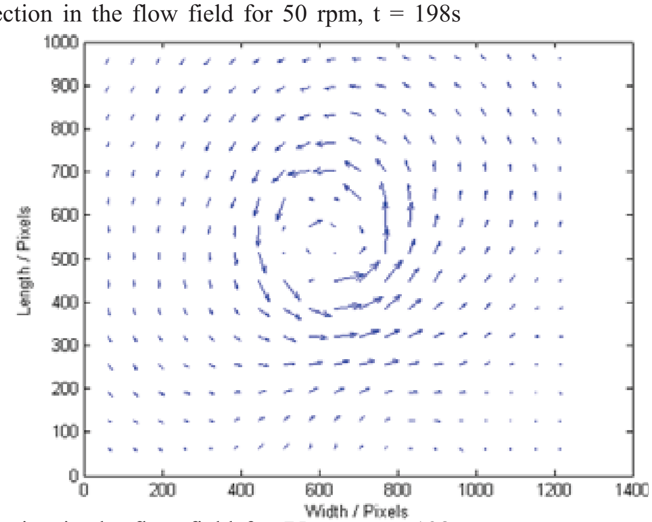

Fig. 16: Particle direction in the flow field for 75 rpm, t = 198s

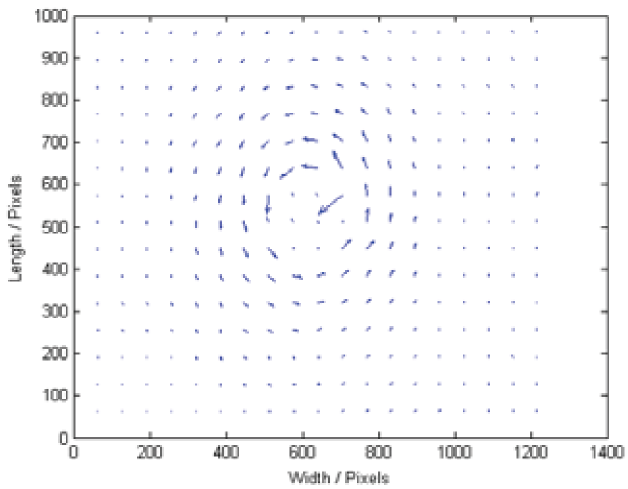

Fig. 17: Particle direction in the flow field for 100 rpm, t = 198s

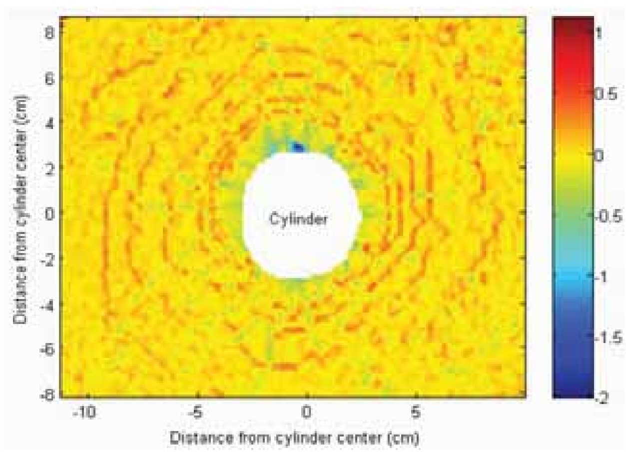

Fig. 18: Vortices distribution in the flow field for 25 rpm, t = 198s. Scale 9:20

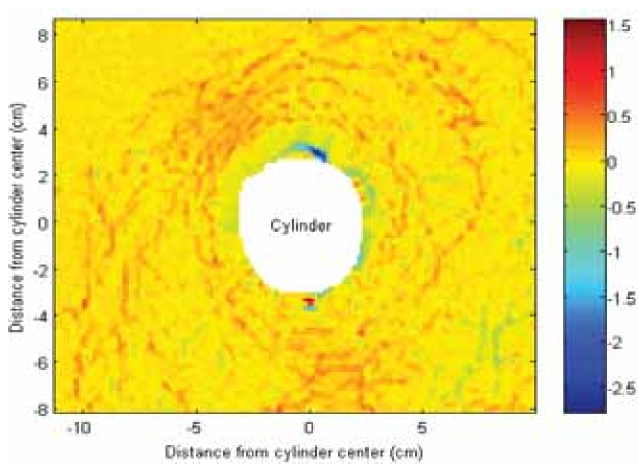

Fig. 19: Vortices distribution in the flow field for 50 rpm, t = 198s. Scale 9:20

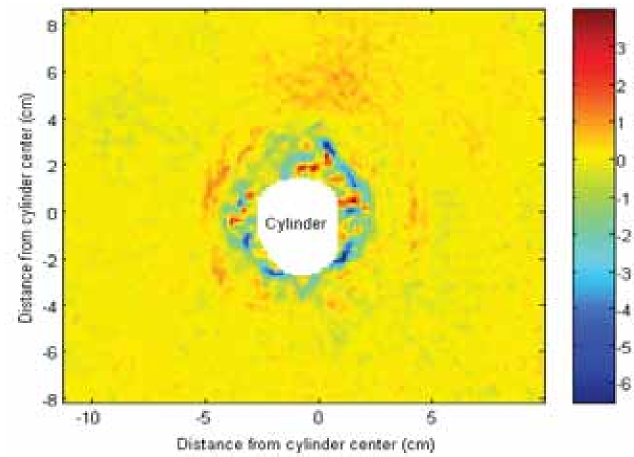

Fig. 20: Vortices distribution in the flow field for 75 rpm, t = 198s. Scale 9:20

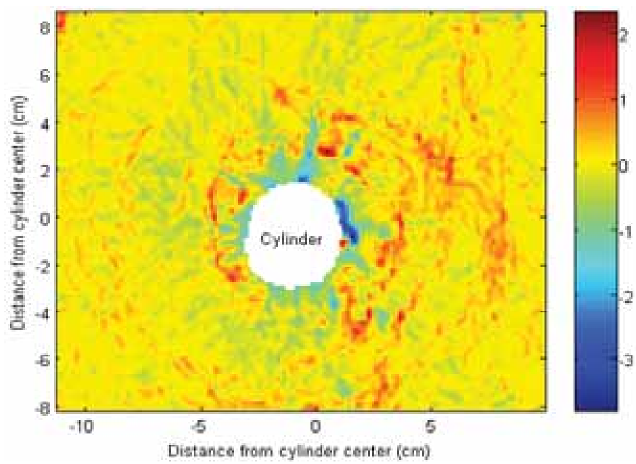

Fig. 21: Vortices distribution in the flow field for 100 rpm, t = 198s. Scale 9:20

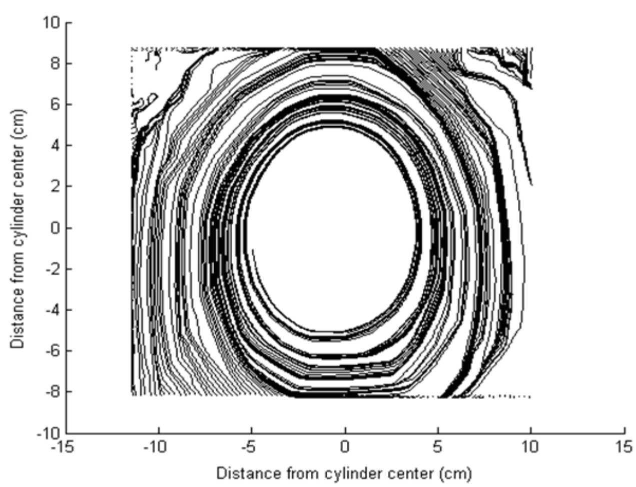

Fig. 22: Streamlines in the flow field for 25 rpm, t = 198s. Scale 9:20

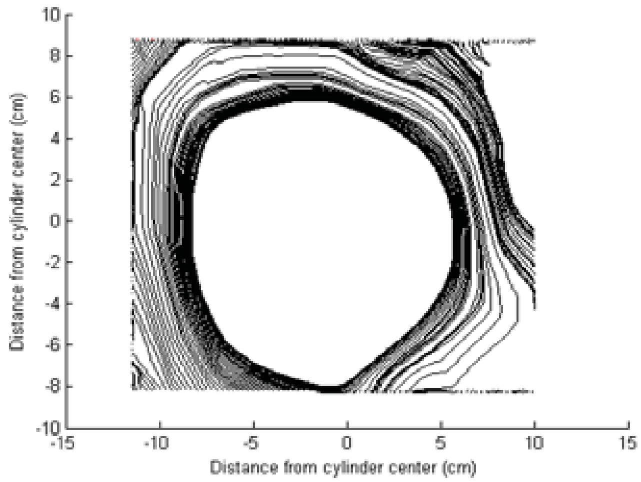

Fig. 23: Streamlines in the flow field for 50 rpm, t = 198s. Scale 9:20

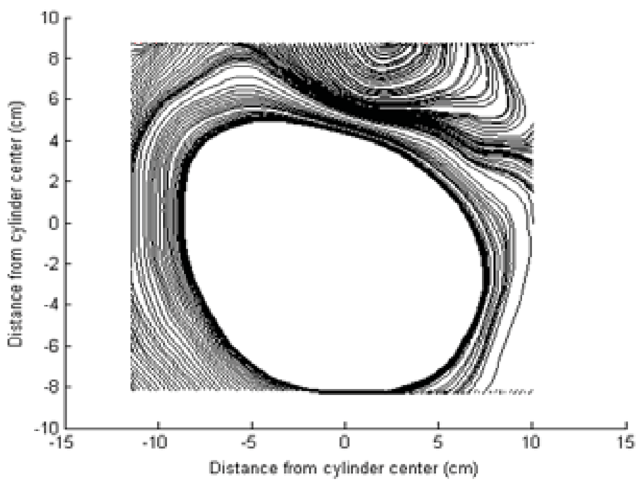

Fig. 24: Streamlines in the flow field for 75 rpm, t = 198s. Scale 9:20

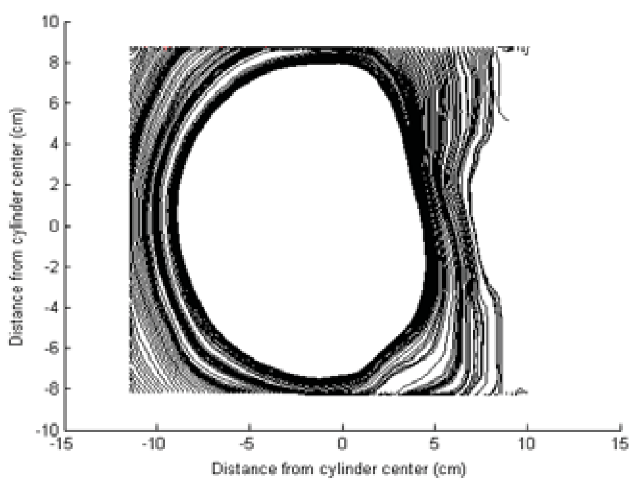

Fig. 25: Streamlines in the flow field for 100 rpm, t = 198s. Scale 9:20

From figure 14 to 17 has discovered particles faction direction in the flow field. Figure 14 provides an idea for particles movement these moves on water surface around a rotating circular cylinder which rotates at 25 rpm and time t = 198s. Consequently figure 15, 16 and 17 illustrates particles movement at 50, 75 and 100 correspondingly and time t = 198s.

Vortices distribution for dissimilar rpm in the flow field are exposed from figure 18 to 21 in fixed time t = 198s. Figure 18 express the vortices distribution at 25 rpm, in this figure vortices quantity is more than at 50 rpm, 75 rpm and 100 rpm flow field subsequent figures are 19, 20 and 21 in that order. All of vortices distribution in the flow field state that vortices exist in the flow field. Increasing cylinder rpm vortices became reduced. Vortices distribution are given away in the scale of 9:20, this scale is the ratio between actual flow field areas which was taken by a digital movie camera to measured areas which was calculated by MatPIV.

Figure 22, 23, 24 and 25 are showing the streamlines for cylinder rpm 25, 50, 75 and 100 likewise, time t = 198s. From these figure we marked that a strong shear layer region exist around rotating circular cylinder. Those shear layer become increasing with the heave of cylinder rpm.

Conclusion:

The average velocity difference between first analytical solution and experimental results are 0.002% for 25 rpm, 0.123% for 50 rpm, 0.469% for 75 rpm and 1.956% for 100 rpm on the other hand, difference between second analytical solution and experimental results are 0.072% for 25 rpm, 0.225% for 50 rpm, 0.650% for 75 rpm and 2.315% for 100 rpm. According to the all figure for 1^{st} analytical solution calculated average velocity we may decide that our 1^{st} analytic solution would be best to explain velocity profile for suddenly starts rotating circular cylinder for time t = 198s. Our future work would be the brief theoretical discussion about velocity distribution, vortices distributions, boundary layer thickness and compare with experimental results with divergent rpm and time condition.

ACKNOWLEDGMENTS

We gratefully acknowledge the help of Mr. A. T. M. Rafiqul Hoque, Assistant Professor, Institute of Forestry and Environmental Sciences, Chittagong University, Chittagong 4331, Bangladesh with several aspects of this paper. Special thanks go to Chief Engineer Mr. T. Q. Choudhury Director, Central Engineering Facilities, Principle Engineer Mr. Mahabubul Haque, Central Engineering Facilities. Extra ordinary appreciation goes to Dr. Silvia Parvez.

REFERENCES

Benton, E.R., 1966. On the flow due to a rotating disk. J. Fluid Mech., 24: 781-800.

Carslaw, H.S., J.C. Jaeger, 1959. Conduction of Heat in Solids, Oxford University Press.

Chia-Shun, Yih, 1969. Fluid Mechanics, A Concise Introduction to the Theory, McGRAW-HILL Book Company.

Collins, W.M., S.C.R. Dennis, 1973. The initial flow past an impulsively started circular cylinder. Q. J. Mech. Appl. Math., 26: 53-75.

Coster. D., 1919. Phil. Mag. 37, pp. 587-594. In: Handbook of Fluid Dynamics, ed. by Jpn. Soc. Fluid Dynamics, Maruzen, Tokyo, (1987).

Grigull, U., H. Sandner, 1986. Warmeleitung, Springer-Verlag, Berlin/Heidelberg.

Johnson, R.W., 1998. The Handbook of Fluid Dynamics, CRC Press, United states.

Schlichting, H., K. Gersten, 2000. Boundary Layer Theory, 8th Revised and Enlarged Edition, Springer.

Streeter, V.L. 1961. Handbook of Fluid Dynamics, First Edition, McGRAW-HILL Book Company Inc..

Tenenbaum, M., H. Pollard, 1963. Ordinary Differential Equations, An Elementary Textbook for Students of Mathematics, Engineering, and Sciences, Dover Publications, Inc., New York.

Appendix I. Notation

a: Cylinder radius [cm]
erf : Error function
$erfc$: Complimentary Error function
J_1: Bessel's function First kind, First order
r: Radial distance from cylinder center [cm]
t: Time [Second]

v_θ: θ - Component velocity
Y_1: Bessel's function Second kind, First order
η: Dimensionless distance
φ: Dimensionless velocity
λ: Eigenvalue
υ: Kinematic Viscosity [cm/s]
ψ: Any arbitrary constant = dφ/dη
Ω: Angular velocity of circular cylinder [rad/s]